

Structure and Dielectric Properties of Cerium Doped Lead Titanate Ceramics

M.Maanan¹, Y.Guaaybess¹, Rahma Adhiri¹, M.Moussetad¹, S.Sayouri², A.Elmesbahi³

¹Laboratory of engineering and material, Faculty of sciences Ben M'sik, Casablanca

²Laboratory of Theoretical and Applied Physics, Faculty of sciences Dhar Mahraz, Fès

³Faculty of sciences and technology, Tanger

Abstract

Sintered ceramic powders of cerium-doped lead titanate ($\text{Pb}_{x/2+1}\text{Ce}_x\text{Ti}_{1-x}\text{O}_3$) ceramics with different Ce dopant concentration in the range ($x=0-0.1$) have been prepared using a sol-gel chemical route. The sol-gel technique is known to offer better purity and homogeneity, and can yield stoichiometric powders with improved properties at relatively lower processing temperature in comparison to conventional solid-state reaction. X-ray diffraction (XRD) scanning electronic microscope (SEM) and Raman spectroscopy studies have been carried out to identify the crystallographic structure and phase formation.

The refinement of the structural parameters was carried out by the Rietveld method. PCT exhibit tetragonal symmetry with the perovskite structure.

The dielectric properties as a function of frequency, and phase transition studies on sintered ceramics $\text{Pb}_{x/2+1}\text{Ce}_x\text{Ti}_{1-x}\text{O}_3$ ($x=0.03$) has been investigated in detail over a wide temperature range 30-500°C and the results are discussed.

Keywords: A. ceramics; B. x-ray diffraction; C. Raman spectroscopy; D. dielectric; C. properties; E. Ce-modified.

Introduction

After the discovery of ferroelectricity in ABO_3 – type perovskite BaTiO_3 , (barium titanate), in 1945, there has been a continuous succession of new materials and technology development

s that have led to a significant number of industrial and commercial applications that can be directly credited to this most unusual phenomenon. Among these applications are high-dielectric-constant capacitors, piezoelectric sonar and ultrasonic transducers, radio and communication filters, pyroelectric security surveillance devices, medical diagnostic transducers, stereo tweeters, buzzers, gasignitors, positive temperature coefficient (PTC) sensors and switches, ultrasonic motors, electrooptic light valves, tri-film capacitors, and ferroelectric thin-film memories.[1]

In recent years, PbTiO_3 (PT) based ferroelectric ceramics have attracted attention due to their high Curie temperature of 490°C and low dielectric constant of about 200. Dielectric and pyroelectric properties of the films and ceramics may be tuned for specific application by appropriate doping. Analysis of the literature shows that among doping elements La [2-8] was the most investigated element. The behavior of other elements of the lanthanide series has been investigated systematically mainly in bulk ceramics. Park et al. [9] prepared and investigated 3mol % of La, Nd, Sm, Gd, Dy, Ho, Er and Yb (Ln in the following) doped PLZT ceramics. Properties of La, Sm and Er modified PZT ceramics were also reported by Pramila et al. [10] and shannigrahi et al. [11]. Pavlovic et al. [12,13] have reported the effect of 50 and 100 mol % of Ce doping on the structure and dielectric properties of bismuth titanate (BT) ceramics.

Properties of Ce modified barium zirconium titanate (BZT) ceramics, Aurivillius-type sodium lanthanum bismuth titanate (NLBT) ceramics were also reported by Feng et al. [14], and Wang et al. [15]. Furthermore, investigation of Ce doping on PbTiO_3 ceramics are still lacking. In a recent work we reported on structural and dielectric properties of Ce doped $\text{Pb}_{x/2+1}\text{Ce}_x\text{Ti}_{1-x}\text{O}_3$ in comparison to non-doped one [16]. The results of the structural characterization demonstrated that the structure does not depend on the concentration of cerium but is sensitive to 14mol% of La doping.

In the present paper emphasis is put on only the effects of cerium doping on the structure and dielectric properties of PbTiO_3 ceramics. Ce doped lead titanate ceramics were obtained by a sol-gel route. The lattice parameters were calculated using XRD analysis. Therefore, we have studied the effect of Ce-modified PT, with one concentration of cerium (3 mol%), on the dielectric constant and loss tangent as well as the transition temperature, and have compared our results to those reported on PLT ceramics and thin films.

1. Experimental

Distilled water, acetic acid and lactic acid based sol-gel method was utilized to fabricate cerium doped lead titanate ceramics with different doping levels. The flow chart diagram on Fig.1 illustrates the process of precursor solutions preparation. Lead acetate, cerium acetate and titanium alkoxide were provided by Fluka chemical, Inc, Germany. 10 mol% of Pb excess were added solution to compensate lead volatility at the subsequent high temperature treatment. $\text{Pb}_{x/2+1}\text{Ce}_x\text{Ti}_{1-x}\text{O}_3$ stoichiometric composition was chosen to calculate the

amount of reagents. 1, 3, 6 and 10 mol% ($x=0.01, 0.03, 0.06$ and 0.1) of Ce was designated to replace Titanate. Lactic acid and distilled water were heated, and after adding titanium isopropoxide a white precipitate is formed, under stirring, at 80°C during 12 hours (peptization), which transforms into clean transparent sol. The stoichiometric amount of corresponding lead acetate and cerium acetate hydrate were dissolved separately in acetic acid and were heated at 80°C for half an hour to remove the water content, and cooled down to 80°C . then stoichiometric amount of transparent sol was added to the solutions in stirring conditions. A small amount of distilled water was added to get the final solution. The mixed solution was kept at 60°C for 48h to get the clear transparent gel. The gel was then dried at 100°C in controlled oven for 72h and then a light brown powder was obtained. The oven dried powder was cold pressed into disks (pellets) using a uniaxial press. The pellets were then sintered for 4h at 1100°C .

Crystalline quality of the powder calcined specimens was studied by X-ray diffraction (XRD). Microstructures of the ceramic samples were analyzed by scanning electron microscopy (SEM). Dielectric constant (ϵ) and dielectric loss ($\tan\delta$) of the samples as a function of temperature (30°C - 500°C) at frequency (100Hz - 1MHz), were obtained using a LCR-meter HP4284A.

2. Results and discussion

3.1 DRX analysis

Phase composition was examined by means of XRD analysis. **Fig. 2** illustrates the X-ray diffraction (XRD) pattern obtained on the prepared Ce-doped lead titanate (PCT) powders by sol-gel technique as a function of varying additive Ce content (0-10 mol%). All the peaks were indexed and lattice parameters were determined and refined using Rietveld method.

The XRD spectra showed distinct peaks corresponding to (001, 100), (101, 110), (111), (002, 200), (102, 201), and (112, 211) planes for all the samples indicating clearly the onset of tetragonal splitting (**Fig. 2**). **Figure 3** shows the XRD pattern of non-doped lead titanate ceramic, which indicates a good crystallization in to the pure tetragonal perovskite phase with no second phase inclusion. The spectrum is very similar to those reported by many research groups for PT ceramics deposited by sol-gel method [17-19]

Compared to pure PT, a small amount of shift is observed in the peak positions indicating a small change in the lattice parameters in Ce-doped PT.

The lattice parameters estimated for these compounds are shown in table1.

| Composition (mol%) | Nature of phase | a (Å) | c(Å) | Unit cell volume(Å ³) | c/a |
|--------------------|-----------------|-------|-------|-----------------------------------|--------|
| 0 | Tetragonal | 3.892 | 4.146 | 62,802 | 1.0652 |
| 1 | | 3.900 | 4.128 | 62,786 | 1.058 |
| 3 | | 3.902 | 4.123 | 62,775 | 1.056 |
| 6 | | 3.902 | 4.123 | 62,775 | 1.056 |
| 10 | | 3.909 | 4.084 | 62,404 | 1.044 |

Table 1: Lattice parameters and unit cell volume of Ce-modified PT ceramic compositions

It is important to note that the value of lattice parameter along c-axis starts decreasing slowly with increase in the value of x, whereas the lattice parameter (a) showed an opposite trend. The results are in agreement with the presence of tetragonal splitting in the XRD spectra as discussed earlier. One can infer that the tetragonality (c/a ratio) in the prepared PCT ceramics decreases from 1,0652 to 1,044 with an increase in x from 0 to 10 mol% respectively (Table1) .

The results indicate that the ceramics are well crystallized into the tetragonal perovskite phase, and that the Ce dopant has no remarkable effect on the structure of lead titanate ceramics.

2.2 SEM micrograph

SEM micrographs of annealed powders at 700°C and bulk ceramic sintered at 1100°C (4h) for PT samples are represented in **figures 4 a and b** respectively.

Grains of PT powders are fine and approximately cubic-shaped, uniformly distributed and very developed. The average diameter of PT particle powder is about 750nm. Dense ceramic with regular size of grains of PT were obtained after sintering pellets at 1100°C for 4 hours as shown on figures 4b, with a domino structure constituted by real spheres which demonstrated the sol-gel process performances. The estimated grain diameter of PT ceramics is $6,7\mu\text{m}$.

2.3 Raman spectroscopy

Raman scattering study is a very sensitive tool for the determination of phase purity and lattice defects [20]. The first-order Raman spectra of tetragonal (L_{4v}) PbTiO_3 have been reported by Burns and Scott [21] and exhibit well – defined phonon modes. There are 12 optic modes in the cubic phase of PbTiO_3 : three triply degenerate T_{1U}

modes (infrared active and Raman inactive), and one triply degenerate T_{2a} mode (Both infrared and Raman inactive). These modes split as in the tetragonal phase.

$$T_{1u} \rightarrow A_1 + E, \quad T_{2u} \rightarrow E + B_1$$

A_1 and E modes split into transverse optic (TO) and longitudinal optic (LO) components by long-range Coulomb forces when propagating along symmetry axes [17]. Fig. 6 shows the Raman scattering spectra recorded on PCT ceramics at room temperature with different values of x .

Fig. 5 shows Raman spectra of crystallized powders of PT. Raman modes of PT have been assigned according to the original work of Burns and Scott [22]. The presence of ten active phonon modes appearing on PT spectrum implies that of the tetragonal phase [21-25]. Low distortion of the tetragonal structure with incorporation of Ce is revealed by a decrease of intensity of the peaks, their shift toward low or high frequencies, and their broadening (Fig. 6).

From structural analyses we can notice, firstly, from XRD analysis, that the change of Ce-doped PT patterns are very small than of PT and, secondly, by examining Raman spectra, we can observe that softening modes $E(1T_0)$ and $E(2L_0)$ localized in Raman spectrum of PT, at 88.6 and 444.9 respectively completely disappear or merge in broadening bands in the case of Ce-doped PT. Thus Ce-doped PT process eight bands instead of ten observed in $PbTiO_3$. Furthermore, Incorporation of cerium does not influence significantly the spectrum corresponding to PT as shown on figure 5.

2.4 dielectric analysis

Dielectric constant and loss tangent as functions of temperature, measured at different frequencies for the samples PCT sintered at 1150°C for 4h are shown in (Fig. 7). With temperature increasing dielectric constant for both Ce-modified PT ceramic with $x=3$ mol% increases and reaches a maximum at around 240°C which is considerably lower than the value of 490°C for pure PT [19]. This is a consequence of the incorporation of Ce in the $PbTiO_3$ lattice which has given rise to a slight crystal lattice distortion.

Loss tangent ($\tan \delta$) decreases with frequency and increases with temperature, with the obvious change in slope at the temperature of the maximum of the dielectric constant (Fig. 8). The loss tangent at 150°C and frequency range between 50 kHz and 1 MHz is inferior to 0.05 for the PCT-3. The increase in the dielectric loss with temperature is correlated with increasing electric and ionic conduction [26].

It should also be noted that strong frequency dispersion is not observed around the dielectric constant peak for the Ce modified sample (Fig. 7). The temperature T_m , corresponding to the maximum value of the dielectric constant, is shifted to higher temperature and the maximum value of the dielectric constant is relatively stable with increasing frequency.

It is well known that the dielectric permittivity of normal ferroelectric above the Curie temperature obeys the Curie-Weiss law described by:

$$\epsilon = \frac{C}{(T - T_{CW})} \quad (T > T_c)$$

Where C is the Curie-Weiss constant and T_{CW} is the Curie-Weiss temperature. In relaxor ferroelectric materials this law is valid only at temperatures much higher than temperature of maximum relative dielectric constant T_m (typically by hundreds of degrees) [27].

Fig. 9 shows the inverse of ϵ as a function of temperature at 200 kHz. The diagram corresponding to PCT3 indicates that far above the Curie temperature dielectric permittivity follows the Curie-Weiss law and at the Curie temperature ϵ has a maximum value ($T_c = T_m$). The fact that the Curie-Weiss temperature T_{CW} of PCT3 ceramic is lower than the Curie temperature transition T_m (Table 2) is expected from the order transition between the paraelectric and ferroelectric phases.

| Samples | $\epsilon_m(T_m)$ | $\tan \delta$ | T_{CW} | $T_m(^{\circ}C)$ | C (Curie Cst.) |
|---------|-------------------|---------------|----------|------------------|-------------------|
| PCT3 | 1412 | 0.05 | 164 | 243 | $0.77 \cdot 10^5$ |

Table 2 – Dielectric parameters of sol-gel – derived PCT3 ceramic at 200 kHz.

Moreover, the value of the Curie-Weiss constant at around $\sim 10^5$ suggests a displacive nature of this transition.

Table 3 gives a comparative study of T_c of PCT and PLCT with those reported in previous studies [16,28] for a percentage of Ce near 3%. Doping of 3% at. of Ce produces a decrease of T_c from 490°C ($PbTiO_3$) to 243°C which is in good agreement with that reported by Gaaaybess [16].

| Samples | xmol%(Ce) | Nature | $T_c (^{\circ}C)$ | Ref. |
|---------|-----------|-----------|-------------------|------------|
| PLT | 3 | Ceramic | 230 | [16] |
| PT | 2 | Thin film | 442 | [28] |
| PT | 3 | Ceramic | 243 | This study |

Table 3. Comparison of Curie temperatures T_c of PLT (14mol% La), PT ceramic and PT thin films

Conclusion

Cerium-modified lead titanate $\text{PbTi}_{1-x}\text{Ce}_x\text{O}_3$ ($x=0-10$ mol%) samples were prepared using the sol-gel process. Structural and microstructural characterizations of the samples were performed using DRX, SEM and Raman spectroscopy. Consequently, the PT ceramic crystallizes in the pure tetragonal structure, while with doping with Ce, a small change in the tetragonal structure of PT occurred at 700°C , without the presence of any secondary phases apart PbO as it was added in excess in the departing materials to compensate its volatilization during heat treatments. A very good texture was obtained for the sample sintered at 1100°C . Dielectric measurements performed on PCT3 ceramic displays one anomaly in the temperature range of $30-500^\circ\text{C}$. This anomaly situated at 243°C is due to the Curie-Weiss transition. The curie transition exhibits a relatively broad peak, however, the paraelectric behaviour of this sample remains governed by a simple Curie-Weiss law, Besides, the value of the Curie-Weiss constant suggest a displacive nature of this transition.

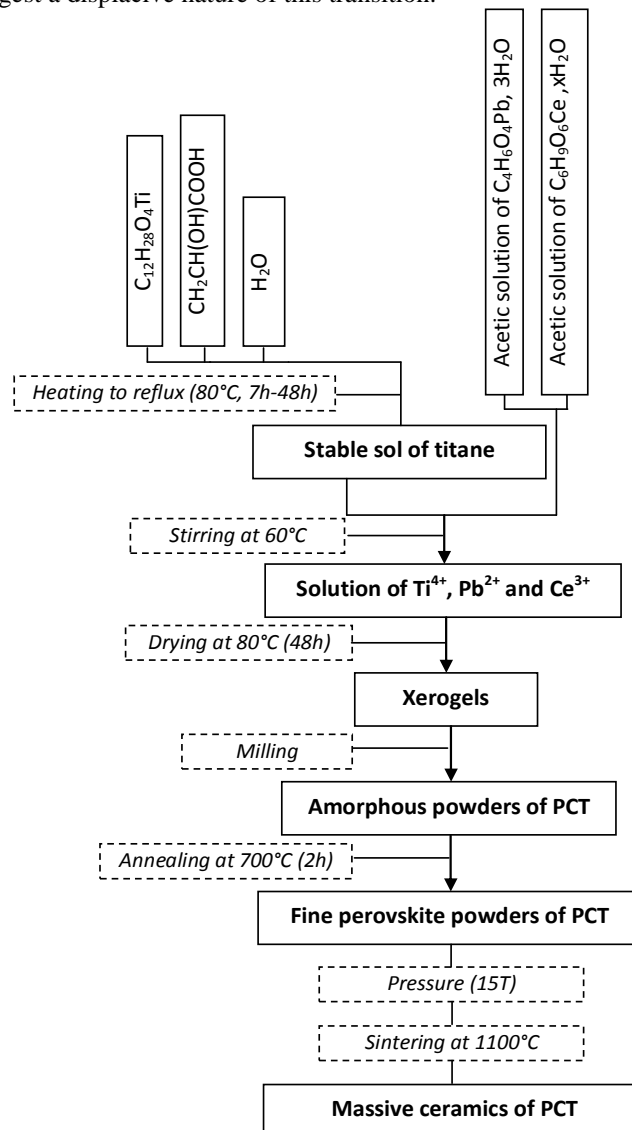


Fig.1. Flow chart for the preparation of PCT ceramics.

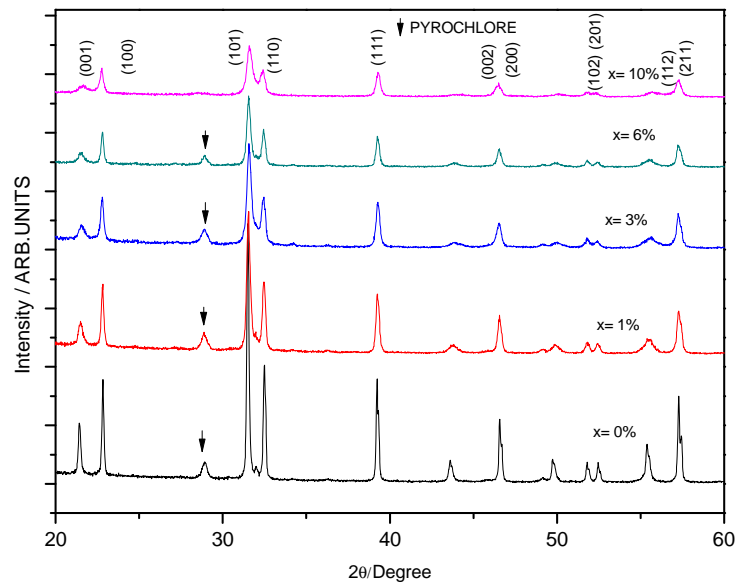


Fig. 2 - X-ray powder diffraction pattern of (a) pure PT, (b) 1%, (c) 3%, (d) 6%, and (e) 10% Ce-doped PT ceramics.

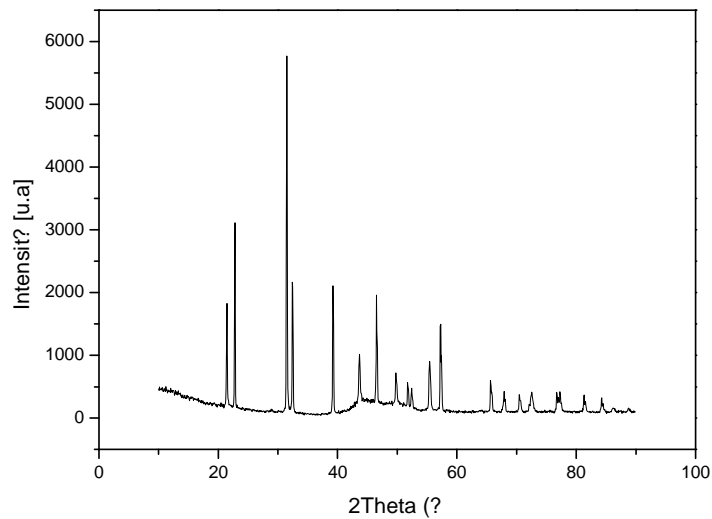
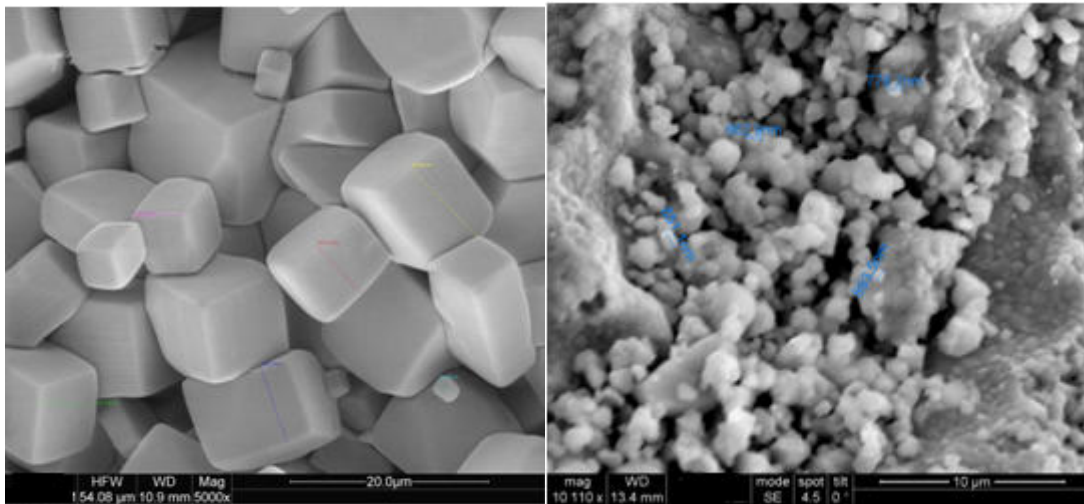


Fig.3- X-ray ceramic diffraction pattern of pure PT



(a) (b)
Fig.4- SEM micrographs of PT annealed powder at 700°C (a) and sintered pellets (1100°C) (b).

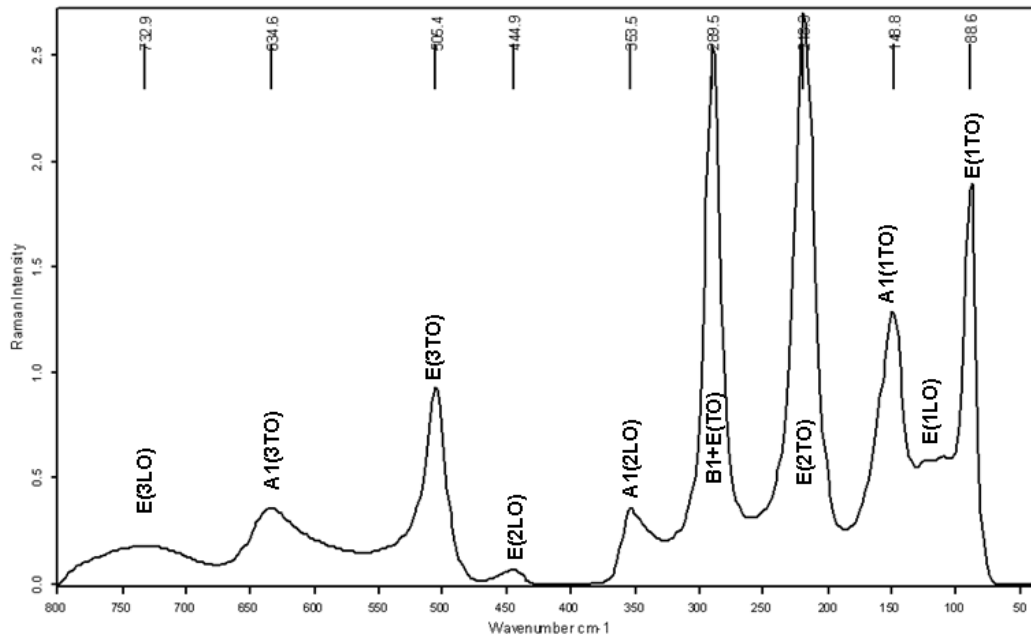


Fig.5: Raman spectra of PT annealed at 700°C.

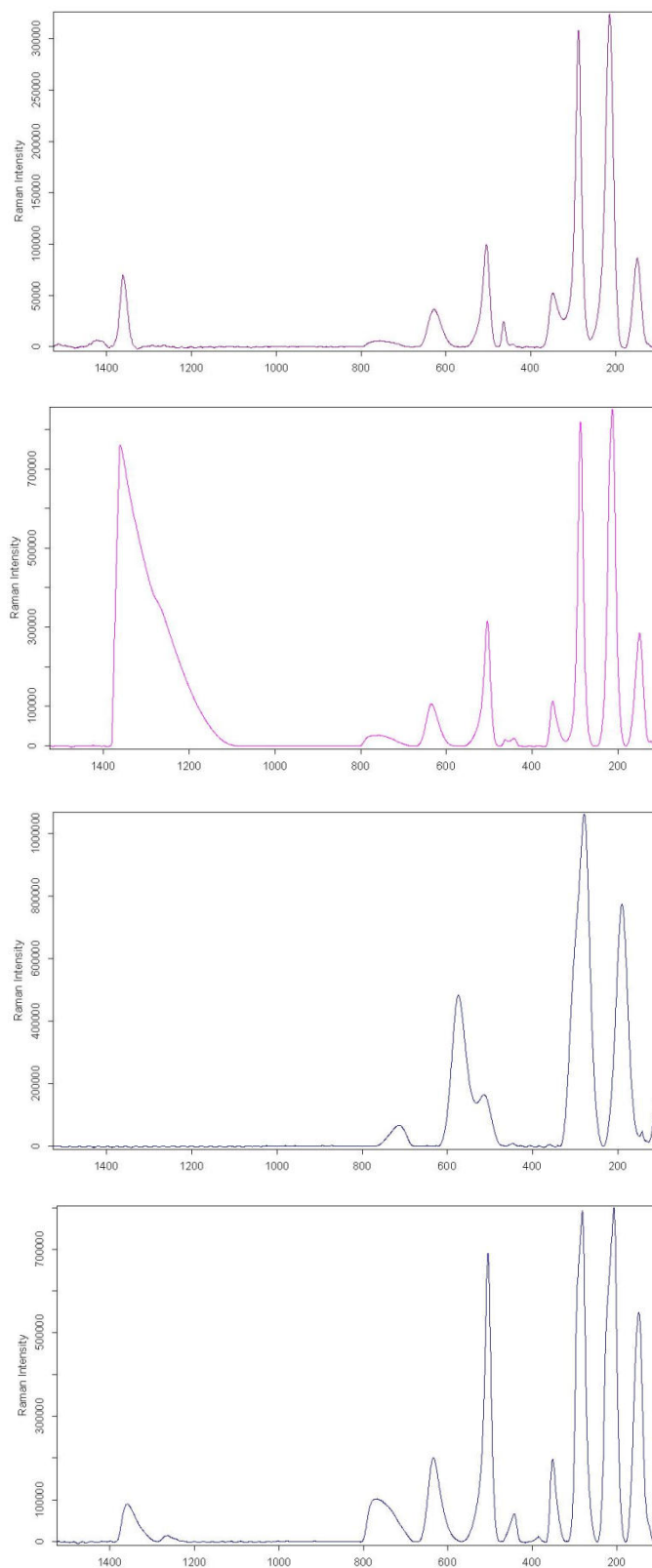


Fig.6- Raman spectra of PCT1 (a), PCT3 (b), PCT6 (c) and PCT10 (d) ceramic

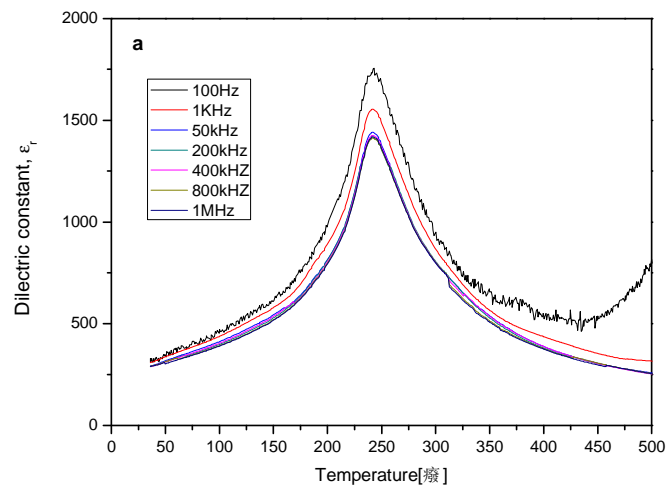


Fig.7 – Dielectric constant of PCT3 as a function of temperature, for seven frequencies.

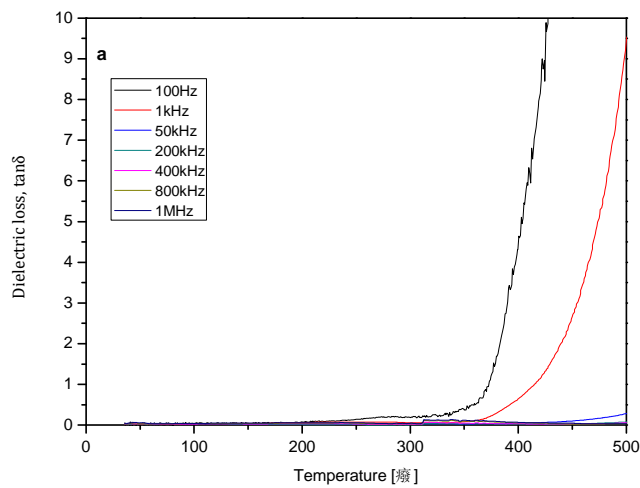


Fig.8 – Dielectric loss tangent of PCT3 as a function of temperature, for seven frequencies.

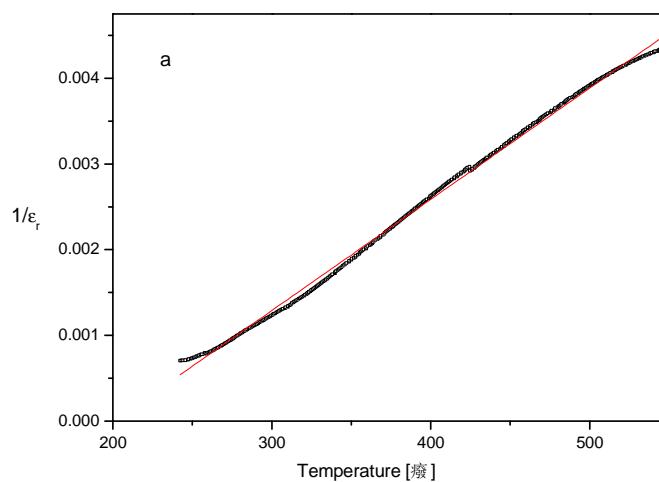


Fig. 9- Inverse dielectric constant at 200 kHz as a function of temperature for PCT3.

References:

- [1] G.H.Haertling, *J.Am. Ceram. Soc.*, 82(4), (1999) 797-818.
- [2] M.Alguero, M.L.Calzada, L.Parda, *J.Mater. Res.*, 14 (1999) 4570.
- [3] Y.-K.Tseng, K.-S.Liu, J-D.Jiang, I.-N.Ling, *Appl.Phys.lett.*, 72(1998) 3285.
- [4] Y.M.Kang, J.K. Ku, S.baik, *J.Appl.Phys.*, 78(1995)2601.
- [5] Y.Guaaybess, M.Moussetad, A.Elmesbahi, S.Sayouri, M.Maanan, R.Adhiri, L.Hajji, O.Azaroual, *Phys-Chem. News*, 53(2010) 34-38.
- [6] A.Elmesbahi, A.Khebeche, S.Sayouri, *J.Catal. Mat.Env.*, 11(2003) 51-54.
- [7] S.B.Majumder, M.jain, R.S.Katigar, *Thin Solid Films*, 402(2002)90-98.
- [8] M.Kellati, S.Sayouri, N.El Moudden, M.Elaatmani, A.Kaal, M.Taibi, *Materials Research Bulletin*, 39(2004)867-872.
- [9] H.-B.Park, C.Y.Park, Y-S.Hong, K.Kim, S.-J.Kim, *J.Am. Ceram.Soc.*,82(1998)94.
- [10]C.Pramila, T.C.Goel, P.K.C.Pillai, *J.Mater.Sci.Lett.*,12(1998)1657.
- [11]S.R.Shannigrahi, R.N.PChoudhary, H.N.Achertya, *Mater.Res.Bull.*,34(1999)1875.
- [12] N.Pavlovic, V.Kolval, J.Dusza, V-V.Srdic, *Ceramics Intertional*, 37(2011)487-492.
- [13] N.Pavlovic, V-V.Srdic, *Materials Research Bulletin*, 44(2009)860-864.
- [14] H.F, J.H, Y.Q, D.S, G.Y, *Journal of alloys and compounds* 512(2012)12-16.
- [15] C-M.Wang, L.Z, J-F.W,L-M.Z, J.D, M-L.Z, C-L.Wang, *Materials science and engineering B* 163(2009)179-183.
- [16] Y. Gaaaybess, M. Maanan, R. Adhiri, M. Moussetad, A. El Mesbahi, S. Sayouri, L. Zarhouni, *MATEC Web of Conferences* 5, (2013) 04036
- [17] A.Singh, V.Gupta, K.Sreenivas, R.S.Katiyar, *Journal of physics and chemistry of solids* 68(2007) 119-123.
- [18] A. Elmesbahi, A. Khebeche, S. Sayouri, *J. Catal. Mat. Env*, 11, (2003)51-54.
- [19] Y. Gaaaybess, M. Moussetad, A. Elmesbahi, S. Sayouri, M. Maanan, R. Adhiri, L. Hajji, O. Azaroual. *Phys-Chem. News*, 53(2010) 34-38.
- [20] V.Gupta, P.Bhattacharya, R.S. Katiyar, M. Tomar, K. Sreenivas, *J. Mater. Res.* 19(8) (2004) 2235.
- [21] G.Burns, Bruce, A. Scott, *Phys. Rev. Lett.* 25(1970) 1191.
- [22] G.Burns, B. A. Scott, *Phys. Rev. B*7(1973)3088.
- [23] W.D. Yang, *Ceram. Int.* 27, (2001) 373-384.
- [24] C.Sanchez, J.Livage, M.Henry, F.Babonneau, *J. Non-Cryst. Solids* 100(1988) 65-76.
- [25] P. S. Dobal, S. B. Mjumder, R. S. Bhaskar, R. S. Katiyar, *J. Rman Spectrosc.* 30(1999) 567.
- [26] A.Q. Jiang, G.H. Li, L.D. Zhang, *Dielectric study in nanocrystalline Bi4Ti3O12 prepared by chemical coprecipitation*, *J. Appl. Phys.* 83 (1998) 4878-4882.
- [27] O.G. Zaldivar, A.P. Barranco, F.C. Pinar, R.L. Noda, L.V. Molina, *A relaxation model by using a relaxation times distribution for relaxor ferroelectrics*, *Scripta Mater.* 55 (2006) 927-930.
- [28] S.Iakovlev, C-H.Solterbeck, M.Es-souni, *Journal of electroceramics*, 10 (2003) 103-110.

The IISTE is a pioneer in the Open-Access hosting service and academic event management. The aim of the firm is Accelerating Global Knowledge Sharing.

More information about the firm can be found on the homepage:
<http://www.iiste.org>

CALL FOR JOURNAL PAPERS

There are more than 30 peer-reviewed academic journals hosted under the hosting platform.

Prospective authors of journals can find the submission instruction on the following page: <http://www.iiste.org/journals/> All the journals articles are available online to the readers all over the world without financial, legal, or technical barriers other than those inseparable from gaining access to the internet itself. Paper version of the journals is also available upon request of readers and authors.

MORE RESOURCES

Book publication information: <http://www.iiste.org/book/>

Recent conferences: <http://www.iiste.org/conference/>

IISTE Knowledge Sharing Partners

EBSCO, Index Copernicus, Ulrich's Periodicals Directory, JournalTOCS, PKP Open Archives Harvester, Bielefeld Academic Search Engine, Elektronische Zeitschriftenbibliothek EZB, Open J-Gate, OCLC WorldCat, Universe Digital Library, NewJour, Google Scholar

